arXiv:1212.2193v1 [math.AG] 10 Dec 2012

# LINKS ARISING FROM BRAID MONODROMY FACTORIZATIONS

MEIRAV AMRAM, MOSHE COHEN, AND MINA TEICHER

Abstract. We investigate the local contribution of the braid monodromy factorization in the context of the links obtained by the closure of these braids. We consider plane curves which are arrangements of lines and conics as well as some algebraic surfaces, where some of the former occur as local configurations in degenerated and regenerated surfaces in the latter. In particular we focus on degenerations which involve intersection points of multiplicity two and three. We demonstrate when the same links arise even when the local arrangements are different.

## 1. Introduction

Braid monodromy is a tool for studying topologically all kinds of curve configurations on 2-dimensional complex surfaces, or branch curves, and also of plane curves which do not appear as branch curves. These computations fit into a program started by Moishezon-Teicher [22, 23, 24, 25, 26, 27] on using braid monodromy factorization as invariants of connected components of the moduli space of surfaces of general type.

In this paper we consider both plane curves and also branch curves of algebraic surfaces as the ramifications of the projection in order to get equivalences between their monodromies and the closures of the monodromies.

In the case of plane curves, there was much work done considering line arrangements [20] and conic-line arrangements [6, 5, 13].

In the case of branch curves, the work of Moishezon-Teicher motivates the classification of algebraic surfaces by developing invariants which differentiate between the components of the moduli space.

This work is followed by the degenerations and regenerations of surfaces and then heavy enumerations of objects in the degenerated surfaces and computations of monodromy and related groups. Degenerations and regenerations of surfaces are tools to make these calculations more manageable; they are used in, for example, [8, 9, 10, 14, 15, 18].

In order to reduce these technical steps we find in this paper equivalences between various degenerations via the resulting monodromies. We use a courser invariant theory by taking their closures, translating the problem to knot and link theory, through which we can say the braids are distinct when the links obtained are distinct.

The overall objective in this context is to understand the building blocks of the braids that appear in the braid monodromy factorization. This leads to a deeper understanding of factorizations that can possibly occur which in turn may shed light on the type of surfaces arising.

In the case of a plane curve, we construct the table of monodromy of Moishezon-Teicher and consider the closures of braids obtained in this way. In the case of a branch curve, we embed an algebraic surface $X$ in a projective space, and we study its degeneration into a union of planes $X_0$. Ordering the edges and vertices in $X_0$ lexicographically [22] and in other ways, we get multiple intersection points which are known from [1, 22, 26] as $k$-points, where $k$ is the number of edges meeting at the vertex. In this paper we focus on 2- and 3-points. Projecting $X_0$ onto $\mathbb{CP}^2$, we get a line arrangement $S_0$ and using the regeneration rules [26], we recover $S$ the branch curve of $X$, used to compute the braid monodromy factorization. See for example [1, 2, 3, 11].

As the braid monodromy technique gives us the braid monodromy factorization of $S$, it is an invariant which distinguishes between connected components of the moduli space. We note that when we consider the affine part of the curves and compute the monodromy, we do not get the braid monodromy factorization but its part without the braids of the singularities at infinity.

From the perspective of knots, we investigate the braids in the braid monodromy factorization by way of local intersection points in the algebraic surfaces and categorize its building blocks. We plan to give a complete list for higher multiple intersection points and expect to obtain new local orderings in deformations of surfaces to answer various questions in algebraic geometry.

This paper contributes to the eventual classification of algebraic surfaces. We implement the closures of the braids to make it easier to understand some known examples. By studying these as links, more simplification can be done. We consider link invariants such as the number of components and the linking numbers between these components; we simplify further by reducing cables until the links we obtain appear on the Knot Atlas [17] as prime. We demonstrate that the same building blocks appear in several of these examples, and this local information will be used to build larger degenerated surfaces. The degeneration pictures (seen in Figures 12, 18, 23, 27, and 18) contain only the affine part, and this is why we ignore the singularities at infinity. These similarities are difficult to recognize at the level of the braids, especially before the computations needed to simplify them.

The paper is organized as follows. In Section 2 we recall plane curves and the braid monodromy that can be obtained from the different singularity types. We give alternate notations for braids, knots, and links. In Section 3 we compute monodromies and their closures that are related to plane curves coming from line arrangements and conic-line arrangements, and we find equivalences between some configurations in Propositions 7 and 8. In Section 4 we introduce the notion of degeneration and consider the different types of 2- and 3-points that arise under different enumerations of the vertices and lines in the degenerations. In Section 5 we compute the related monodromies and their closures for all types of 2- and 3-points. In addition to these local contributions we also consider global symmetries in Proposition 27. In Section 6 we give interesting examples of regenerations of 2-points and 3-points and the results concerning their braids and closures. We show that the closures of monodromies of all types of 2-points are the same. This holds also for one type of 3-points: in the regeneration process we get two double lines and one conic. The second type of 3-points is the exceptional case: in the regeneration process we get two conics and one double line, giving only one possible labelling.

## 2. BACKGROUND

We will follow the braid monodromy algorithm of Moishezon-Teicher [23, 24]. A detailed treatment may also be found in [1, 12].

Algebraically a braid is a word in the Artin group $B_m$ generated by $\sigma_1, \dots, \sigma_{m-1}$, where geometrically $\sigma_i$ takes the $i$-th strand over the $(i+1)$-st strand and acts as the identity on the others, as in Figure 1. See also [16].

The element $\sigma_i$ can also be denoted $Z_{i\,i+1}$. This generalizes to $Z_{i\,j}$ as in Figure 2. The reader unfamiliar with the $Z_{i\,j}$ notation may choose to read [23].

*Property* 1. The braids $Z_{i\,j}$ and $\overline{Z}_{i\,j}$ can be re-written as

$$Z_{i\,j} = (\sigma_i \dots \sigma_{j-2})\sigma_{j-1}(\sigma_i \dots \sigma_{j-2})^{-1} = (\sigma_{i+1} \dots \sigma_{j-1})^{-1}\sigma_i(\sigma_{i+1} \dots \sigma_{j-1}),$$

$$\overline{Z}_{i\,j} = (\sigma_{j-2} \dots \sigma_i)^{-1}\sigma_{j-1}(\sigma_{j-2} \dots \sigma_i) = (\sigma_{j-1} \dots \sigma_{i+1})\sigma_i(\sigma_{j-1} \dots \sigma_{i+1})^{-1}.$$

*Property* 2. The braid $Z_{i\,i+1\,\dots\,i+k}$ can be re-written as

$$Z_{i\,i+1\,\dots\,i+k} = (\sigma_{i+k-1} \dots \sigma_i)(\sigma_{i+k-1} \dots \sigma_{i+1}) \dots (\sigma_{i+k-1}\sigma_{i+k-2})(\sigma_{i+k-1}).$$

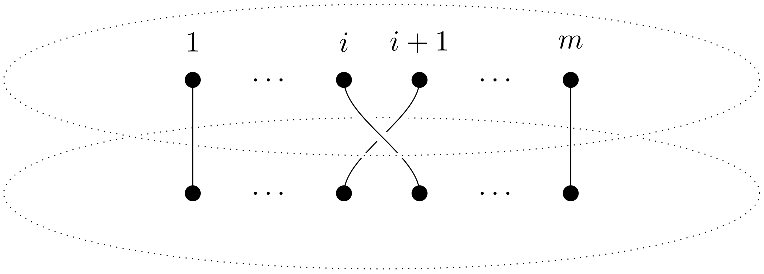

FIGURE 1. The element $\sigma_i$.

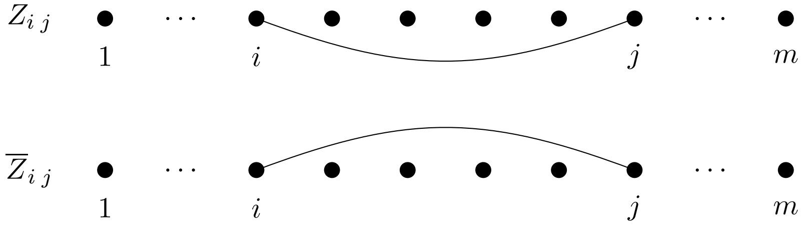

FIGURE 2. The braids associated with $Z_{i\,j}$ and $\overline{Z}_{i\,j}$.

For a more in-depth overview of knots and links, including linking number, see for example [21].

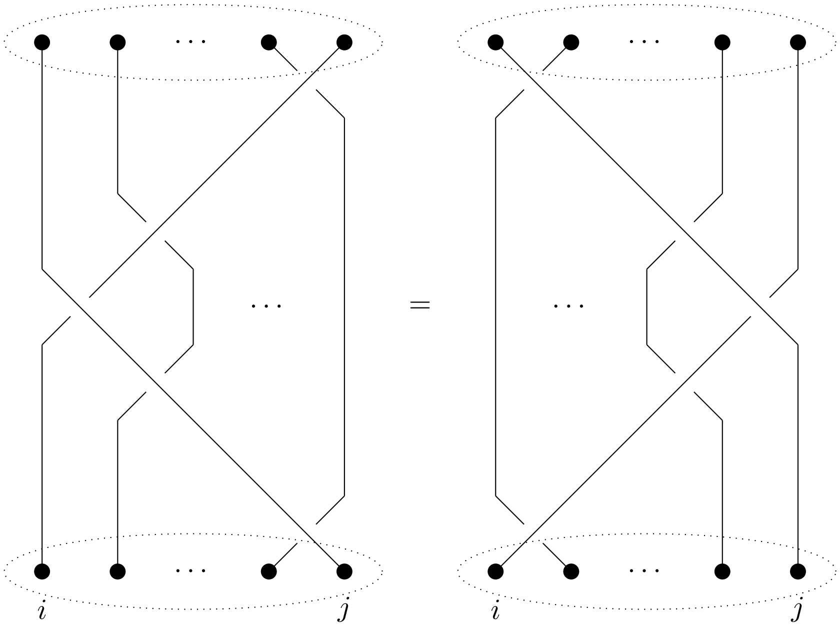

FIGURE 3. The related braid $Z_{i\,j}$.

Braids given by conjugation in the $Z_{i\,j}$ notation can be much more complicated. Figure 4 gives a step-by-step method to determine, for example, the relatively easy conjugation $(Z_{3\,8})^{Z^2_{3\,5}Z^2_{3\,4}}$.

2.1. **Singularity types.** We detail the different types of singularities in a plane curve.

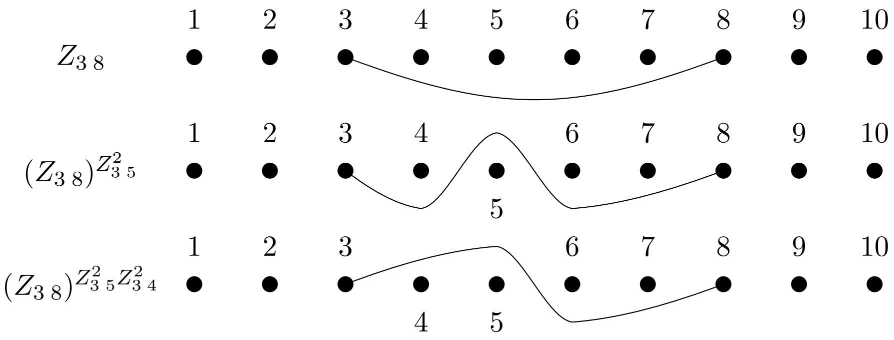

FIGURE 4. An example of a conjugated braid $(Z_{3\,8})^{Z^2_{3\,5}Z^2_{3\,4}}$.

2.1.1. *Branch point.* For convenience here we consider only conics opening to the right as in Figure 5. Note that to the right of the singularity, each typical fiber has two real intersection points. However, to the left of the singularity the intersection points are complex.

The associated exponent $\varepsilon$ of a branch point is 1.

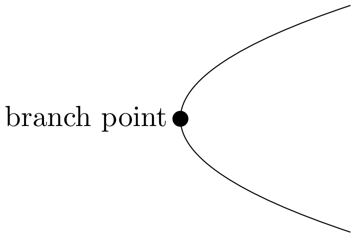

FIGURE 5. The conic and its branch point.

2.1.2. *Node.* A node is the intersection of two components. The associated exponent $\varepsilon$ of a node is 2.

**Example 3.** Consider the arrangement of three lines forming a triangle as in Figure 6.

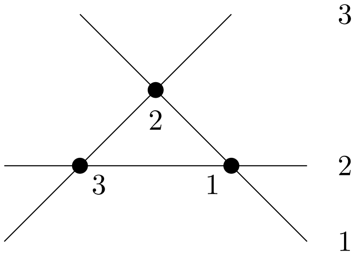

FIGURE 6. An arrangement of three lines.

The braids related to the three nodes are $Z^2_{1\,2}$, $\overline{Z}^2_{1\,3}$, and $Z^2_{2\,3}$. Their product can be expressed as:

$$\sigma_1^2 \cdot (\sigma_1^{-1}\sigma_2\sigma_1)^2 \cdot \sigma_2^2 = \sigma_1\sigma_2^2\sigma_1\sigma_2^2.$$

The closure of this braid is the torus link $T(3,3)$.

2.1.3. *Intersection point at infinity.* The associated exponent $\varepsilon$ of an intersection point at infinity is 2. For several parallel lines, consider the lexicographic ordering of the related braids when multiplying them together (considering the ordering from the right-hand side).

2.1.4. *Tangency.* The associated exponent $\varepsilon$ of a tangency is 4.

In Section 4, we explain in more detail that the regeneration of a tangency yields three cusps, each of whose associated exponent $\varepsilon$ is 3. See [26].

2.1.5. *Intersection points with higher multiplicities $k > 2$.* The associated exponent $\varepsilon$ of an intersection point with multiplicity $k > 2$ is 2. This exchanges the $i$-th and $(i + (k - 1))$-st positions, the $(i + 1)$-st and $(i + (k - 1) - 1)$-st positions, and so on.

## 3. PLANE ARRANGEMENTS WITH LINES AND CONICS

In this section, we consider three kinds of arrangements: first those with only lines, then those with only conics, and then those with both.

First we note that all local arrangements of $m$ lines give the same local contribution to the braid monodromy factorization. In particular, the closure of this braid is the well-studied torus link on $m$ strands twisted $m$ times.

In this section we begin with generic line arrangements, where each pair of lines intersects at exactly one distinct node. From there we consider parallel lines as well as central arrangements, in order to produce the more general case, for example the one seen in Example 6.

Given a generic arrangement of $m$ lines, every pair of lines intersects exactly once, and every intersection point is a node where exactly two lines meet. Then the $\binom{m}{2}$ nodes, each with degree 2, contribute to the total degree $m(m-1)$ of the braid monodromy factorization of $\Delta^2$, which is two full twists on $m$ strands.

**Proposition 4.** *(Moishezon-Teicher)* [23, Proposition-Example VIII.2.1] *For a generic arrangement of $m$ lines, that is, with only double points and with no parallel lines, the braid monodromy factorization is equivalent to (with respect to an equivalent relation that has not been defined in this paper)*

$$\prod_{\ell=2}^{m}\prod_{k=1}^{\ell-1} Z^2_{k\,\ell}.$$

Observe that this is written in some reverse-lexicographic ordering not corresponding to the order of the singularities on the axis.

*Property* 5. Consider the closure of $\Delta^2$ on $m$ strands. This link has the following properties:

1. it has $m$ components,
2. each of the $m$ components is itself unknotted, and
3. each pair of components considered alone is the Hopf link.

Furthermore it is the torus link $T(m, m)$ on $m$ strands twisted $m$ times.

One can also think of the lines on the plane as great circles on the sphere, and with the condition that each node becomes a positive crossing, this achieves the link described above.

Consider next the central arrangement of $m$ lines. Then one need only consider the intersection point with multiplicity $m$ as described above, and the braid monodromy factorization has $\Delta^2$ as its one factor, which was treated in the generic case above. See Property 2.

Now consider the arrangement of $m$ parallel lines. Then the "intersection point at infinity" in the lexicographic order is as described above, and again the braid monodromy factorization has $\Delta^2$ as its one factor. However, this point at infinity will not be considered in the local contribution to the braid monodromy factorization. See the following example.

**Example 6.** Consider the line arrangement in Figure 7 with a triple point and parallel lines.

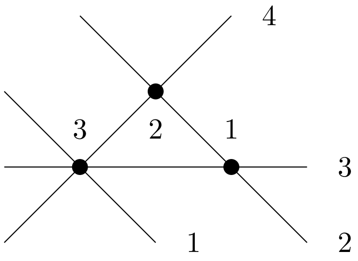

Figure 7. A general example of a line arrangement.

The braid monodromy table is given in Table 1.

Table 1. The braid monodromy table for a more general arrangement of four lines.

| singularity | exponent $\varepsilon$ | related braid |
|---|---|---|
| 1 | 2 | $Z^2_{2\,3}$ |
| 2 | 2 | $\overline{Z}^2_{2\,4}$ |
| 3 | 2 | $Z^2_{1\,3\,4}$ |

The product of the five resulting braids is given in Equation (3.1):

$$\sigma_2^2 \cdot (\sigma_2^{-1}\sigma_3^2\sigma_2) \cdot [\sigma_1(\sigma_3\sigma_2\sigma_3)^2\sigma_1^{-1}] = \sigma_2\sigma_3\sigma_1\sigma_2(\sigma_1\sigma_2\sigma_3)^2. \tag{3.1}$$

A horizontal depiction of this braid is given Figure 8.

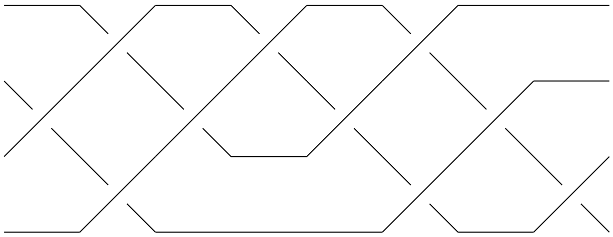

Figure 8. The braid obtained from Example 6.

The closure of this braid gives a link of four components, each of which is itself an unknot with no crossings. The intersection point at infinity, which is not included here in this local contribution, would link the first two components. All other pairs have linking number one.

This link can also be interpreted as the Hopf link L2a1 on the Thistlethwaite Link Table on the Knot Atlas [17] whose first component unknot is replaced by its (2,0)-cable and whose second component unknot is replaced by its (2,2)-cable. Recall that a $(p, t)$-cable has $p$ parallel copies and $t$ twists.

Next we consider some arrangements of conics and lines together. In particular, some of these appear in the local partial regenerations of surfaces as in Section 4.

**Proposition 7.** *Consider the two arrangements of a single conic and a single line shown in Figure 9.*

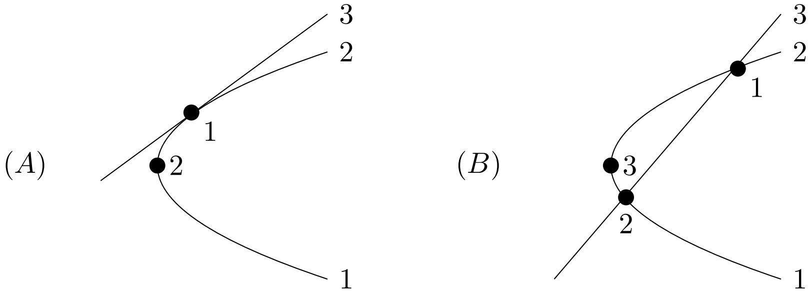

FIGURE 9. Two arrangements of a single conic and a single line.

*Then the braids given by the local contribution of the braid monodromy factorization are the same. Furthermore, the link obtained by the closure of this braid is the torus link $T(2,4)$. This is also the alternating link L4a1 on the Thistlethwaite Link Table on the Knot Atlas* [17] *as shown in Figure 10.*

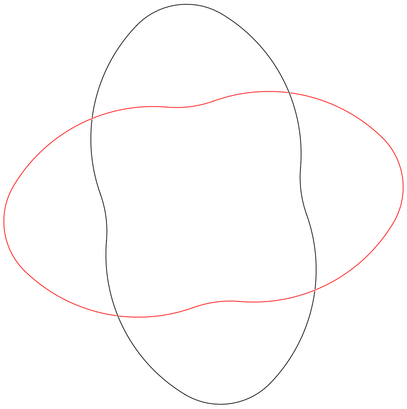

FIGURE 10. The alternating link L4a1.

*Proof.* Consider the arrangement of a single line tangent to a single conic as in Figure 9 (A). The braid monodromy table for just these two points gives $Z^4_{2\,3}$ and $(Z_{1\,2})^{Z^2_{2\,3}}$, contributing locally $\sigma_2^4 \cdot (\sigma_2^{-2}\sigma_1\sigma_2^2) = \sigma_2^2\sigma_1\sigma_2^2$.

Alternatively one could slide the line of this arrangement so that it passes through the conic twice as in Figure 9 (B), creating two nodes and the branch point. Here the resulting braids are $Z^2_{2\,3}$, $Z^2_{1\,3}$, and $Z_{1\,2}$, which contribute the product $\sigma_2^2 \cdot (\sigma_2^{-1}\sigma_1^2\sigma_2) \cdot \sigma_1 = \sigma_2\sigma_1^2\sigma_2\sigma_1 = \sigma_2^2\sigma_1\sigma_2^2$ like above.

After a stabilization move, the braid is $\sigma_2^4$, whose closure is $T(2,4)$. $\square$

Next we consider some arrangements of conics only. Observe that Figure 11 (B) appears in the partial regeneration of the 3-point with the second type as considered in Example 19 and Figure 14 (II).

**Proposition 8.** *Consider the two arrangements of two conics shown in Figure 11.*

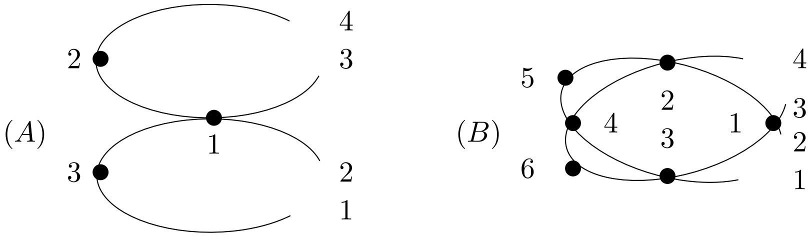

FIGURE 11. Two conic arrangements.

*Then the first link obtained by the closure of the braids given in the local contribution to the braid monodromy factorization is L4a1 as on* [17] *as shown in Figure 10, and the second is L4a1 with one component replaced with its (2,1)-cable.*

*Proof.* Consider the arrangement of two conics with a single tangency along with the two branch points as in Figure 11 (A). The braid monodromy table for these three points gives the related braids $Z^4_{2\,3}$, $(Z_{3\,4})^{Z^2_{2\,3}}$, and $(Z_{1\,2})^{Z^2_{2\,3}}$ contributing locally $\sigma_2^4 \cdot (\sigma_2^{-2}\sigma_3\sigma_2^2) \cdot (\sigma_2^{-2}\sigma_1\sigma_2^2) = \sigma_2^2\sigma_3\sigma_1\sigma_2^2$. After two stabilization moves on the closure, this gives the same as the closure of $\sigma_2^4$ on two strands, which is the four-crossing alternating link L4a1 on [17] as shown in Figure 10.

Alternatively consider the arrangement of two conics with no tangencies, giving four nodes along with the two branch points as in Figure 11 (B). The braid monodromy table for these six points gives the related braids $Z^2_{2\,3}$, $\overline{Z}^2_{2\,4}$, $Z^2_{1\,3}$, $(Z^2_{1\,4})^{Z^{-2}_{3\,4}}$, $Z_{3\,4}$, and $Z_{1\,2}$. Together these contribute

$$\sigma_2^2 \cdot (\sigma_3\sigma_2^2\sigma_3^{-1}) \cdot (\sigma_2^{-1}\sigma_1^2\sigma_2) \cdot (\sigma_3\sigma_2^{-1}\sigma_1^2\sigma_2\sigma_3^{-1}) \cdot \sigma_3 \cdot \sigma_1$$

$$= \sigma_2\sigma_3^2\sigma_1^2\sigma_2\sigma_3\sigma_1\sigma_2^2, \tag{3.2}$$

whose closure is the same as $\sigma_2\sigma_1^3\sigma_2\sigma_1^3\sigma_2$ on three strands after a stabilization move and some conjugation. This gives a two-component link where each component interacts as in L4a1 on the Knot Atlas [17] but where one component unknot is replaced with its (2,1)-cable. Recall that a $(p,t)$-cable has $p$ parallel copies and $t$ twists.

This is also the two-component link where each component interacts as in the Hopf link L2a1 on the Knot Atlas [17] but where each component replaced with its (2,1)-cable. ☐

*Remark* 9. The arrangements which appear in Figures 9 and 11 are the affine pieces of the projective arrangements. The projective arrangements are not themselves interesting because they yield the complete braid monodromy factorization, which always gives the torus link $T(m,m)$.

## 4. SURFACES

Let $X$ be an algebraic surface embedded in projective space $\mathbb{CP}^n$. Projecting $X$ onto the projective plane $\mathbb{CP}^2$ we get its branch curve $S$, that is, the ramification locus of the projection.

In order to better understand the complicated branch curve $S$, we degenerate the surface $X$. A partial degeneration gives a union of squares, each of which is homeomorphic to $\mathbb{CP}^1 \times \mathbb{CP}^1$, using horizontal and vertical lines. Each square is further degenerated into two planes by adding diagonal lines to obtain a union $X_0$ of triangles representing planes. A detailed explanation of the degeneration process may be found in [25] and in further work including [1, 7, 10, 12], for example. We take the following definition from [1].

**Definition 10.** Let $D$ be the unit disc, and $X, Y$ be algebraic surfaces (or more generally algebraic varieties). Suppose that $k : Y \to \mathbb{CP}^n$ and $k' : X \to \mathbb{CP}^n$ are projective embeddings. We say that $k'$ is a *projective degeneration* of $k$ if there exist a flat family $\pi : V \to D$, and an embedding $F : V \to D \times \mathbb{CP}^n$, such that $F$ composed with the first projection is $\pi$, and:

(a) $\pi^{-1}(0) \simeq X$;
(b) there is a $t_0 \neq 0$ in $D$ such that $\pi^{-1}(t_0) \simeq Y$;
(c) the family $V - \pi^{-1}(0) \to D - 0$ is smooth;
(d) restricted to $\pi^{-1}(0)$, $F = 0 \times k'$ under the identification of $\pi^{-1}(0)$ with $X$;
(e) restricted to $\pi^{-1}(t_0)$, $F = t_0 \times k$ under the identification of $\pi^{-1}(t_0)$ with $Y$.

To demonstrate we explain this process for the degeneration of the Hirzebruch surface $F_2(1,2)$ into six planes (the triangles) in Figure 12. There are five lines separating the six planes once we ignore the boundary. The intersections of these five lines occur at six points, four of which has multiplicity two and so are called 2-points (as marked by black vertices in the figure) and two of which are called 1-points (as marked by white vertices). We project $X_0$ onto the plane and obtain a branch curve $S_0$ depicted by these five lines with these six intersection points. In order to recover the original branch curve $S$ of $X$, we must regenerate $S_0$.

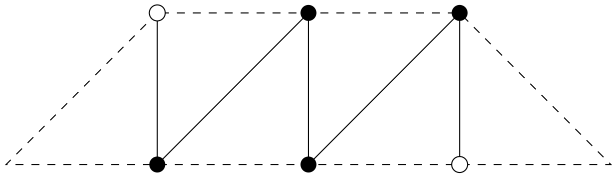

FIGURE 12. The Hirzebruch surface $F_2(1,2)$ degenerated into six planes.

Now we explain in general the regeneration process, for any branch curve $S_0$. The degenerated branch curve $S_0$ has degree say $m$. However each of the $m$ lines of $S_0$ should be counted as a double line in the scheme-theoretic branch locus, since it arises from a line of nodes. Another way to see this is to note that the regeneration of $X_0$ induces a regeneration of $S_0$ in such a way that each point, say $c$, on the typical fiber is replaced by two nearby points $c, c'$. The resulting branch curve $S$ will have degree $2m$.

In full generality the branch curve $S_0$ has $k$-points as intersections for any $k$. The regeneration process for large $k$ can be quite difficult, but work has been done for some values: see [19], [12], and [4] for 5-, 6-, and 8-points, respectively. In this work we restrict our attention to regenerations of just 2- and 3-points.

We show in Subsections 4.1 and 4.2 that different types of these $k$-points arise based on different orderings of the lines. These line orderings are determined by orderings on the vertices. In additional to the common lexicographic ordering, others are given.

The lines intersecting at these $k$-points are horizontal, vertical, or diagonal based on the construction from squares and triangles. In the regeneration process we do not differentiate between horizontal and vertical lines; these will eventually regenerate into double lines. On the other hand, diagonal lines will regenerate into conics. We are concerned with intersections of these lines and conics. The following lemma from [26] explains how tangencies arise in the regeneration process.

**Lemma 11.** *(Moishezon-Teicher)*[26] *Let $V$ be a projective algebraic surface, and $C'$ be a curve in $V$. Let $f : V \to \mathbb{CP}^2$ be a generic projection. Let $S \subseteq \mathbb{CP}^2, S' \subset V$ be the branch curve of $f$ and the corresponding ramification curve. Assume $S'$ intersects $C'$ at a point $\alpha'$. Let $C = f(C')$ and $\alpha = f(\alpha')$. Assume that there exist neighborhoods of $\alpha$ and $\alpha'$, such that $f_{|_{S'}}$ and $f_{|_{C'}}$ are isomorphisms. Then $C$ is tangent to $S$ at $\alpha$.*

We start with a regeneration of 2-points. A diagonal line in a 2-point is regenerated to a conic which is tangent to the horizontal or vertical line, as in Lemma 11 and Figure 13. In the partial regeneration we get a curve with a tangency and a branch point. In order to complete the regeneration process, the line is doubled and the tangency is regenerated to three cusps.

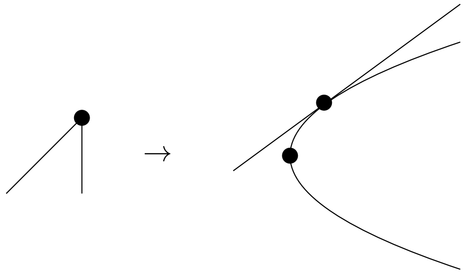

FIGURE 13. Partial regeneration in a neighborhood of a 2-point.

Now we study the regeneration of 3-points. The three intersecting lines can be horizontal, vertical, or diagonal, and one might suspect that any configuration is possible. Due to the construction by squares, however, there can be no 3-point with no diagonals and no 3-point with all diagonals. Thus there are two types of 3-points, as in Figure 14.

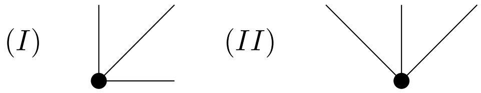

FIGURE 14. The two types of a 3-point.

For the first type, the regeneration is divided into steps. We explain each step in two levels, first dealing with the surface and then with the branch curve. At the surface level, each diagonal is replaced with a conic by a partial regeneration. Focusing on a 3-point, we have a partial regeneration of two of the planes to a quadric surface. We get one quadric and one plane, which is tangent to the quadric. The plane and the quadric meet along two lines (one from each ruling of the quadric). At the branch curve level, we have two double lines (coming from the intersection of the plane and the quadric) and one conic (coming from the branching of the quadric over the plane). According to Lemma 11, the conic is tangent to each of the two double lines. As far as the branch points go, one of the two branch points of the conic is far away from the 3-point, and the other one is close to the 3-point. See Figure 15.

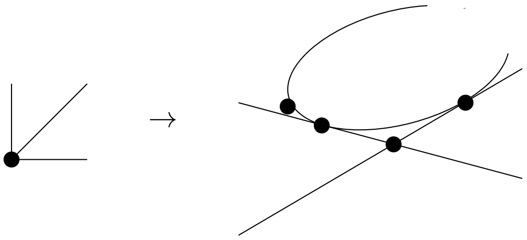

FIGURE 15. Partial regeneration in a neighborhood of the 3-point of the first type.

In the next step of the regeneration, at the curve level, we use regeneration lemmas from [24]. The two tangent points regenerate to three cusps each (giving a total of six) and the intersection point of the two double lines gives eight more branch points. One can think of this as first giving four nodes, then each node giving two branch points. At the surface level it means that we get a smooth surface which locally looks like a cubic in $\mathbb{CP}^3$ (degenerating to a triple of planes).

Now we study the regeneration of the second type of a 3-point. One of the diagonal lines regenerates to a conic which is tangent to the vertical line. The vertical line and the second diagonal line (which is still yet to be regenerated) intersect at a 2-point. In the second step of the regeneration, the second diagonal line is regenerated to a conic which is tangent to the vertical line, too. See Figure 16.

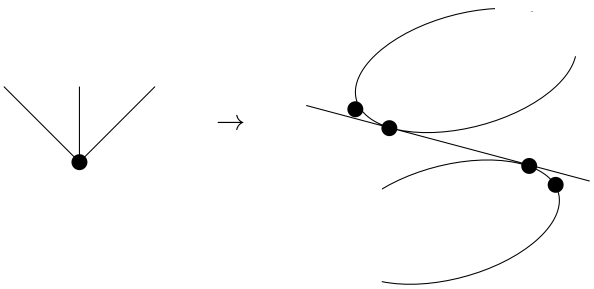

Figure 16. Partial regeneration in a neighborhood of the 3-point of the second type.

In the last step, the vertical line is doubled and each tangency regenerates to three cusps. Note that the two conics intersect in four complex points (not shown).

Now we formulate the regenerated braid for a node and for a tangency using the regeneration rules from [26].

Recall that the braid $Z^2_{ij}$ is a full-twist of $j$ around $i$ and the braid $Z^2_{i'j}$ is a full-twist of $j$ around $i'$. The braid $Z^2_{ii',j}$ is obtained by a regeneration (the point $i$ on the typical fiber is replaced by $i, i'$), and it is a full-twist of $j$ around $i$ and $i'$.

**Theorem 12. Regeneration rule for a node** *(Moishezon-Teicher)* [26, p. 337]
*A factor of the form* $Z^2_{ij}$ *regenerates to* $Z^2_{ii',j}$, $Z^2_{i,jj'}$ *or* $Z^2_{ii',jj'}$.

In the last case, the regeneration of a node can be depicted as in Figure 17.

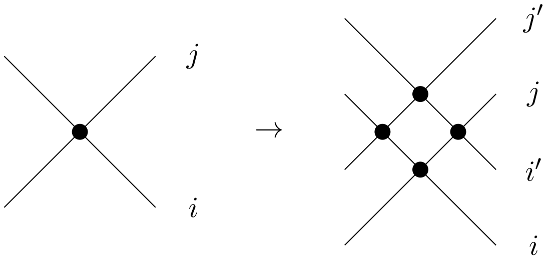

Figure 17. Regeneration of a node.

These three cases are explicitly given by (a), (b), and (f) of the following lemma:

**Lemma 13.** *(Amram-Teicher)* [12, Lemma 10] *The following hold: (a)* $Z^2_{ii',j} = Z^2_{i'j}Z^2_{ij}$*; (b)* $Z^2_{i',jj'} = Z^2_{i'j'}Z^2_{i'j}$*; (c)* $Z^{-2}_{i',jj'} = Z^{-2}_{i'j}Z^{-2}_{i'j'}$*; (d)* $\bar{Z}^{-2}_{i',jj'} = \bar{Z}^{-2}_{i'j'}\bar{Z}^{-2}_{i'j}$*; (e)* $Z^{-2}_{ii',j} = Z^{-2}_{ij}Z^{-2}_{i'j}$*; (f)* $Z^2_{ii',jj'} = Z^2_{i',jj'}Z^2_{i,jj'}$*; (g)* $Z^{-2}_{ii',jj'} = Z^{-2}_{i,jj'}Z^{-2}_{i',jj'}$*.*

Recall that a tangency is regenerated into three cusps.

**Theorem 14. Regeneration rule for a tangency** *(Moishezon-Teicher)* [26, p. 337] *A factor of the form* $Z^4_{ij}$ *regenerates to* $Z^3_{i,jj'} = (Z^3_{ij})^{Z_{jj'}} \cdot (Z^3_{ij}) \cdot (Z^3_{ij})^{Z_{jj'}{}^{-1}}$ *or to* $Z^3_{ii',j} = (Z^3_{ij})^{Z_{ii'}} \cdot (Z^3_{ij}) \cdot (Z^3_{ij})^{Z_{ii'}{}^{-1}}$*.*

Next we consider 2- or 3-points that appear in degenerations of surfaces.

4.1. **Degeneration and regeneration of 2-points.** 2-points appear in degenerations as intersections of two lines. We can find them in degenerations of Hirzebruch surfaces, in a self-product of the projective line, in a product of the projective line with a complex torus, or in some toric varieties. In Figure 18, for example, we show a degeneration of the surface $\mathbb{CP}^1 \times \mathbb{CP}^1$, embedded by the bi-linear system (1,2). The black vertices in the figure are 2-points.

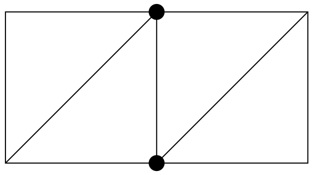

FIGURE 18. The 2-points in the surface $\mathbb{CP}^1 \times \mathbb{CP}^1$.

The ordering on the degenerated surface is determined by an ordering on the vertices. There are several ways of doing this, but the most convenient one is the lexicographic ordering following work by Moishezon and Teicher. Consider vertices $v_1 = (x_1, y_1)$ and $v_2 = (x_2, y_2)$. Then $v_1 < v_2$ if and only if $y_1 < y_2$ or $y_1 = y_2$ and $x_1 < x_2$. That is, enumerate vertices starting from the lower left corner proceeding to the right and then continuing upwards. Consider lines $L_1$ through vertices $u_1$ and $v_1$ and $L_2$ through vertices $u_2$ and $v_2$ under the condition that $u_1 < v_1$ and $u_2 < v_2$. Then $L_1 < L_2$ if and only if $v_1 < v_2$ or $v_1 = v_2$ and $u_1 < u_2$. For example, the vertices and the lines of Figure 18 can be enumerated as in Figure 19.

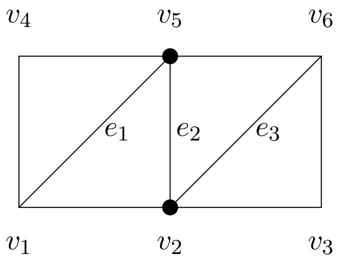

FIGURE 19. Enumerations of lines and vertices.

Choose a 2-point arbitrarily. By the regeneration lemmas in [24], the diagonal line is regenerated to a conic which is tangent to the line as in Figure 20. This figure shows the two possibilities of partial regeneration, depending on the ordering of the components.

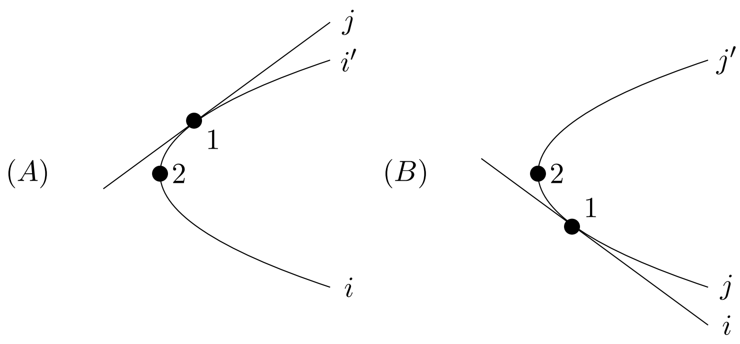

Figure 20. Two cases of partial degeneration of a 2-point.

*Remark* 15. Observe that the possibility in Figure 20 (A) occurs as the vertex labelled $v_5$ in Figure 19 and the possibility in Figure 20 (B) occurs as the vertex labelled $v_2$.

In order to complete the regeneration process, each tangent line is regenerated to two parallel lines, and the tangency is replaced by three cusps (following the regeneration rules of [26]).

By the Moishezon-Teicher table of monodromy, we can compute the braids which are related to the singularities in Figure 20, and then by the above rule we get a curve of degree 4 with three cusps and a branch point of a conic. Figure 21 (A1) and (B1) are related to the three cusps which we get from the tangency in Figure 20 (A) and (B), respectively. Figure 21 (A2) and (B2) are related to the branch point of the conic in Figure 20 (A) and (B), respectively.

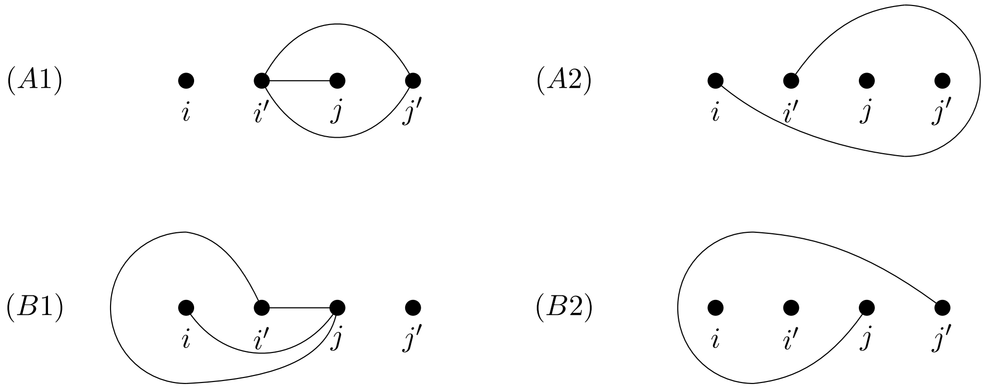

Figure 21. Braids related to 2-point cases with $j = i + 1$.

4.2. **Degeneration and regeneration of 3-points.** A 3-point in a degeneration is an intersection of three lines. We consider two types as in Figure 14: one that regenerates into two lines and a conic and the other that regenerates into one line and two conics. We consider each type at a time, demonstrating what orderings of the three lines are possible and showing examples.

Let us consider a 3-point of the first type in a degenerated surface as in Figure 14 (I).

**Proposition 16.** *Given a 3-point of the first type, any ordering of the three lines $i$, $j$, and $k$ can be obtained by the lexicographic ordering of the vertices in the degenerated surface, as shown in Figure 22.*

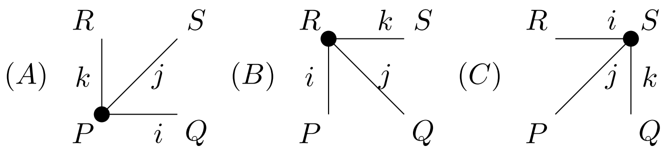

FIGURE 22. Possible orderings of edges around a 3-point of the first type.

*Proof.* Following Figure 22, we assign coordinates to the vertices $P = (x_1, y_1)$, $Q = (x_2, y_1)$, $R = (x_1, y_2)$, and $S = (x_2, y_2)$ with $x_1 < x_2$ and $y_1 < y_2$.

In Figure 22 (A), this gives the ordering of the lines as $i < k < j$, in Figure 22 (B), this gives $i < j < k$, and in Figure 22 (C) this gives $j < k < i$. ☐

**Example 17.** Consider the "(2, 2)-pillow degeneration" of a $K3$ surface of degree 16 which is embedded in $\mathbb{CP}^9$, appearing in [1] and shown in Figure 23. The boundaries of the two pieces are identified with the left piece on top and right piece on bottom. Observe that the ordering of the vertices is not purely lexicographic because of identifications of the edges giving non-planarity. Here the boundary points $v_1$ to $v_8$ are labelled *in this order* using the lexicographic ordering while the interior point on the top is $v_9$ and the bottom is $v_{10}$. this gives $v_1 < \ldots < v_8 < v_9 < v_{10}$. The corner vertices $v_1$, $v_3$, $v_6$, and $v_8$ are the 3-points that appear as Figure 22 (A).

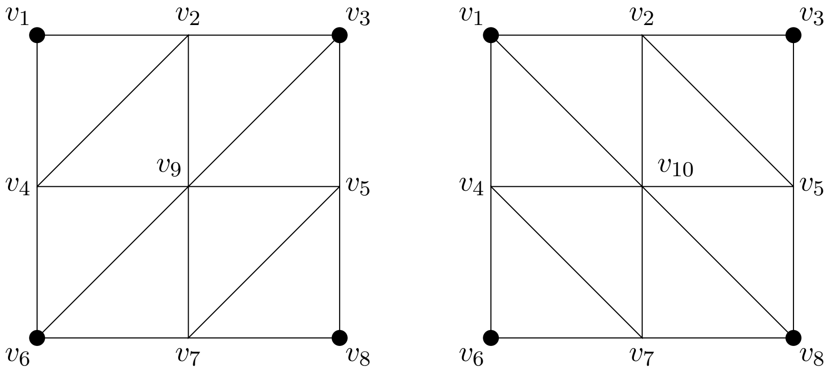

FIGURE 23. The (2, 2)-pillow degeneration.

Next we consider another ordering of the same pillow degeneration given in [18]. Here the boundary points $v_1$ to $v_8$ are ordered *clockwise* $v_1 < v_2 < v_3 < v_5 < v_8 < v_7 < v_6 < v_4$. However, the four corner vertices are the same 3-points that appear in Figure 22 (A).

Now consider the complete lexicographic ordering on the first piece that starts from the bottom left corner: $v_6 < v_7 < v_8 < v_4 < v_9 < v_5 < v_1 < v_2 < v_3$ followed by $v_{10}$ on the other piece. Contrasting with the earlier two orderings, only $v_1$ and $v_8$ appear in Figure 22 (A) while $v_6$ appears in Figure 22 (B) and $v_3$ appears in Figure 22 (C)!

In Figure 24 we present the three cases of the first type of 3-point for three arbitrary indices $i, j, k$, where $i < j < k$.

In the regeneration process, the diagonal line is regenerated into a conic which is tangent to both lines. In the next step, each line of the two lines is regenerated into two parallel lines, causing the appearance of three cusps instead of each tangency point. Moreover, each node is regenerated into four nodes as in Figure 25. Suppose that two lines intersect at a node, say lines $i$ and $j$. Recall from Lemma 13 that the resulting braid is $Z^2_{i\,i',j\,j'} = Z^2_{i'\,j'} Z^2_{i'\,j} Z^2_{i\,j'} Z^2_{i\,j}$.

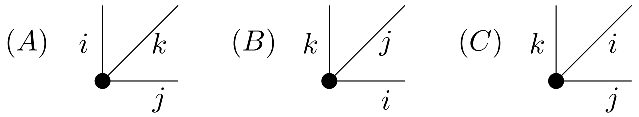

FIGURE 24. 3-points of the first type with $i < j < k$.

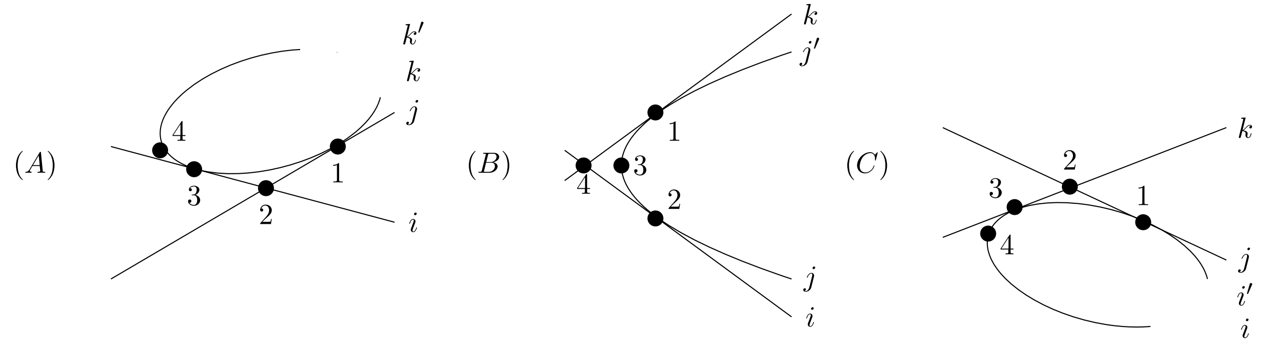

FIGURE 25. Partial regeneration of the 3-point cases with $i < j < k$.

**Proposition 18.** *Given a 3-point of the second type, the only ordering of the three lines obtained by the lexicographic ordering of the vertices is* $i \leq j \leq k$ *as shown in Figure 26.*

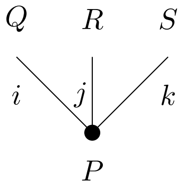

FIGURE 26. The only 3-point case for the second type ordering with $i < j < k$.

*Proof.* Following Figure 26, we assign coordinates to the vertices $P = (x_2, y_1)$, $Q = (x_1, y_2)$, $R = (x_2, y_2)$, and $S = (x_3, y_2)$ with $x_1 < x_2 < x_3$ and $y_1 < y_2$. Following the enumeration of vertices, we conclude that we have the enumeration of lines $i < j < k$. $\square$

**Example 19.** Consider the surface $\mathbb{CP}^1 \times \mathbb{CP}^1$. Take $l_1 = \mathbb{CP}^1 \times pt$ and $l_2 = pt \times \mathbb{CP}^1$. For $a, b \in \mathbb{N}$, consider the linear combination $al_1 + bl_2$. We embed our surface into a projective space with respect to the linear system $|al_1 + bl_2|$.

For this example we take $a = 1$ and $b = n$ as in Figure 27. Enumerating the vertices in a purely lexicographic manner $v_1 < v_2 < \ldots < v_{2n+2}$, we obtain the black vertices $v_2, v_4, \ldots, v_{n-1}$ and $v_{n+4}, v_{n+6}, \ldots$ that are 3-points of the second type.

To obtain a second example, we extend the degeneration of the bi-embedding (1,2) of $\mathbb{CP}^1 \times \mathbb{CP}^1$ to a degeneration of a singular toric surface embedded in $\mathbb{CP}^6$ as in [10] and shown in Figure 28. Here the purely lexicographic ordering of vertices $v_1 < v_2 < \ldots < v_7$ gives a 3-point of the second type – the black vertex labelled $v_2$.

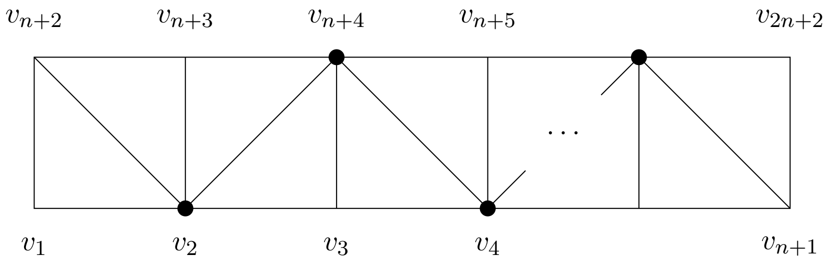

Figure 27. A degeneration of $\mathbb{CP}^1 \times \mathbb{CP}^1$ with $a = 1$ and $b = n$.

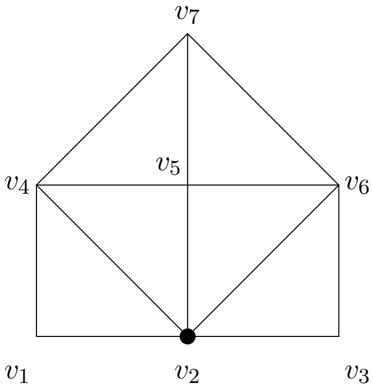

Figure 28. A degeneration of a singular toric surface embedded in $\mathbb{CP}^6$.

## 5. Main Results

The overall goal of Subsection 5.1 is to translate local information from the degeneration of the curve to local information in the resulting braid obtained by the braid monodromy algorithm presented by Moishezon-Teicher [24]. In the first setting we consider the components that meet at each singularity, and in the second setting we consider strands of the braid. Proposition 20 states that these global indices are in fact the same across both settings. Proposition 21 shows that the order of these singularities does not affect the braiding.

The main result in Subsection 5.2 is Proposition 27, which relates a global transformation of the curve to a global transformation of the resulting braid.

These results provide us with the ability to classify the closures of the links obtained from 2-points and 3-points in Section 6.

### 5.1. Local contributions to the braid monodromy.

Our first goal is to prove that the indices of the components of the curve meeting at a singularity (in local configurations) tell us where the braiding occurs when considering all strands.

**Proposition 20.** *The global indices $i$ and $j$ of the two components of the curve that meet at a local singularity are the global indices of the strands in the resulting braid for that local singularity.*

*Proof.* Recall that the singularity can be viewed locally as the curve $y^2 = x^\varepsilon$ for $\varepsilon = 1, 2, 3, 4$ giving, respectively, a branch point, a node, a cusp, and a tangency. The resulting local braid monodromy for such a singularity is $\phi = Z^{\varepsilon}_{i\,i+1}$ as in Moishezon-Teicher [23, p.487 Proposition-Example VI.1.1.][23, p.487 Proposition-Example VI.1.1.].

This singularity appears in the regeneration of some $k$-point (for $k = 2, 3$), where we recall that we get only branch points, nodes, and cusps. This $k$-point contributes $\beta_{2k}$, where $2k$ is the degree of the local regeneration as well as the number of strands in this braid, to the overall braid monodromy factorization, and we embed $\phi \hookrightarrow \beta_{2k}$.

The construction of $\beta_{2k}$ is determined by the regeneration of the embedding of braid groups $B_k \hookrightarrow B_n$ into $B_{2k} \hookrightarrow B_{2n}$, where the index of $B$ is the number of strands of the braid, and recall that $n$ is the number of lines in the projection of the degenerated surface $X_0$ to $S_0$.

Then we have $\phi \hookrightarrow \beta_{2k} \hookrightarrow \Delta^2_{2n}$, where the braid monodromy factorization contributes $\Delta^2_{2n}$ globally. Thus the end points maintain their indices. □

Next we take this local information obtained from the singularity and show that it is unaffected by other singularities.

**Proposition 21.** *The local contribution to the resulting braiding of the strands indexed by Proposition 20 is unaffected by the order in which the singularity is considered in the braid monodromy process.*

*Proof.* The locally contributed braid $\beta$ can be written as a product $\beta_1, \ldots, \beta_k$ of braids. The individual conjugations $\alpha^{-1}\beta_i\alpha$ together give the single conjugation $\alpha^{-1}\beta\alpha$, thus leaving $\beta$ intact.

Any additional strands that come into $\beta$ in $\alpha^{-1}$ leave in $\alpha$ in the opposite way. Thus in the closure the components related to the additional strands do not become linked with the components coming from $\beta$. In particular, these strands can themselves be conjugated to return back to the identity. □

In the regeneration process, each indexed component $i$ in the branch curve of $n$ components becomes two components $i$ and $i'$. In braid notation on $2n$ strands, these correspond to strands $2i - 1$ and $2i$, as in the following proposition.

**Proposition 22.** *The following products of braids correspond to Figure 21 (A1), (A2), (B1), (B2) respectively, which depict cusps and branch points.*

$$(Z^3_{i'\,i+1})^{Z_{i+1\,i+1'}} \cdot Z^3_{i'\,i+1} \cdot (Z^3_{i'\,i+1})^{Z^{-1}_{i+1\,i+1'}} = (\sigma^{-1}_{2i+1}\sigma^3_{2i}\sigma_{2i+1}) \cdot \sigma^3_{2i} \cdot (\sigma_{2i+1}\sigma^3_{2i}\sigma^{-1}_{2i+1}) \tag{5.1}$$

$$(Z_{i\,i'})^{Z^2_{i',\,i+1\,i+1'}} = (\sigma_{2i}\sigma^2_{2i+1}\sigma_{2i})^{-1}\sigma_{2i-1}(\sigma_{2i}\sigma^2_{2i+1}\sigma_{2i}) \tag{5.2}$$

$$(Z^3_{i\,i+1})^{Z_{i\,i'}} \cdot Z^3_{i\,i+1} \cdot (Z^3_{i\,i+1})^{Z^{-1}_{i\,i'}} = \sigma^3_{2i} \cdot (\sigma^{-1}_{2i}\sigma^3_{2i-1}\sigma_{2i}) \cdot (\sigma^2_{2i-1}\sigma^3_{2i}\sigma^{-2}_{2i-1}) \tag{5.3}$$

$$(Z_{i+1\,i+1'})^{Z^2_{i+1,\,i\,i'}} = (\sigma_{2i}\sigma^2_{2i-1}\sigma_{2i})^{-1}\sigma_{2i+1}(\sigma_{2i}\sigma^2_{2i-1}\sigma_{2i}) \tag{5.4}$$

*Proof.* According to the regeneration rule for tangency (Theorem 14) we get the left hand sides of the equations. Using Property 1 we get the right hand sides.

The product of the three braids in 5.1 and 5.3 corresponds to the three cusps in Figure 21 (A1) and (B1) respectively. These can be simplified to $\sigma_{2i}\sigma^3_{2i+1}\sigma_{2i}\sigma^3_{2i+1}\sigma_{2i}$ and $\sigma_{2i}\sigma^3_{2i-1}\sigma_{2i}\sigma^3_{2i-1}\sigma_{2i}$ respectively. Moreover, we get the braids in 5.2 and 5.4 corresponding to the branch points in Figure 21 (A2) and (B2) respectively. □

To demonstrate these last few results, consider the following example.

**Example 23.** The braid $(Z_{1\,2})^{Z^2_{2\,4}Z^2_{2\,3}}$ is given in Figure 29.

The resulting braid can be written $(\sigma_2^{-1}\sigma_3^{-2}\sigma_2^{-1})\sigma_1(\sigma_2\sigma_3^2\sigma_2)$. It is clear here that the components indexed by 3 and 4 are unlinked and can be removed by conjugation.

This leads us to the following results on the number of components of the links we obtain. In the proposition above we saw indexed components $i$ and $i'$ in the branch curve. However in several cases these components become a single component in the closure of the related braid. In order to better see this, we present first the following case analysis for branch points, cusps, and nodes.

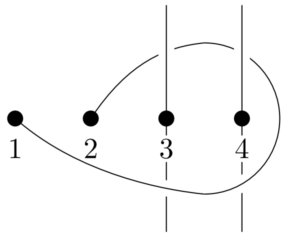

FIGURE 29. The braid given by $(Z_{1\,2})^{Z^2_{2\,4}Z^2_{2\,3}}$.

**Lemma 24.** *A conic indexed by $i$ and $i'$ with a branch point contributes a single component to the link obtained by closing the braid.*

**Lemma 25.** *A line indexed by $j$ and $j'$ (respectively $i$ and $i'$) tangent to a conic at a singularity that regenerates into three cusps contributes a single component to the link obtained by closing the braid; together with the conic $i$ and $i'$ (respectively $j$ and $j'$) this gives two components.*

Recall the regeneration of a node as in Figure 17.

**Lemma 26.** *A single node that regenerates into four nodes contributes four components to the link obtained by closing the braid.*

5.2. **Global contributions to the braid monodromy.** Next we present a statement that will allow us to move between similar cases. Let $S$ be an arrangement in $\mathbb{CP}^2$. It can be a plane curve or a branch curve of a surface $X$ or of one of its degenerations. Let $r(S)$ be the rotation of 180° of $S$ around the horizontal line that is the chosen axis for the ordering of the singularities.

It is natural that the braid monodromy factorization of $r(S)$ is a rotation of the braid monodromy factorization of $S$. Nevertheless it is not written anywhere, and for the sake of clarification for the reader and for coherence we include a proof here.

**Proposition 27.** *The local contributions to the braid monodromy factorization obtained from $S$ and $r(S)$ are related by a rotation around a line parallel to the direction of the braid. Moreover the closures of these braids give the same links.*

For the sake of clarification, we take the braid to be depicted vertically and thus will consider rotation of the braid around a vertical line. However, some of the figures below depict the braids horizontally to conserve space.

*Proof.* First observe that the order of the singularities in $S$ is preserved by the rotation. So we need only consider a single singularity. We start by considering only a partial regeneration in which we have a branch point, simple node, or tangency. Afterwards we continue to a complete regeneration where a simple node is regenerated into four nodes and tangency is regenerated into three cusps.

Suppose components $i$ and $j$ meet at a singularity. The resulting braid from the braid monodromy algorithm is a conjugation of $Z^{\varepsilon}_{i\,j}$, where $\varepsilon$ is the exponent associated to the type of singularity as in [24]. By Property 1, $Z_{i\,j}$ can be rewritten as

$$Z_{i\,j} = (\sigma_i \dots \sigma_{j-2})\sigma_{j-1}(\sigma_i \dots \sigma_{j-2})^{-1} = (\sigma_{i+1} \dots \sigma_{j-1})^{-1}\sigma_i(\sigma_{i+1} \dots \sigma_{j-1}). \tag{5.5}$$

In $r(S)$ the components that meet at the associated singularity are numbered $(n+1)-i$ and $(n+1)-j$.

Now let us consider the local contribution to the braid monodromy obtained from this singularity in $r(S)$. This braid is a conjugation of some $Z^{\varepsilon}_{(n+1)-j\;(n+1)-i}$, where $\varepsilon$ is the exponent associated to the type of singularity as in [24]. By Property 1, this can be re-written as

$$
\begin{aligned}
(5.6)\quad Z_{(n+1)-j\ (n+1)-i} &= (\sigma_{(n+1)-j}\cdots\sigma_{(n+1)-i-2})\sigma_{(n+1)-i-1}(\sigma_{(n+1)-j}\cdots\sigma_{(n+1)-i-2})^{-1}\\
&= (\sigma_{(n+1)-j+1}\cdots\sigma_{(n+1)-i-1})^{-1}\sigma_{(n+1)-j}(\sigma_{(n+1)-j+1}\cdots\sigma_{(n+1)-i-1}).
\end{aligned}
$$

A rotation of some generator $\sigma_k^{\pm 1}$ around a vertical line is $\sigma_{n-k}^{\pm 1}$. Thus we can see that Equations 5.5 and 5.6 are related by a reflection around a vertical line. In this way this rotation also holds for any conjugation, as this conjugation can be expressed in terms of the $\sigma_i$'s.

Having proved the partial regeneration, we move to the complete regeneration. For the case of a branch point, we apply Proposition 20 to the regeneration where some point $i$ becomes two points $i$ and $i'$. The next two lemmas consider the cases of a single node and a tangency.

**Lemma 28.** *For the case of a single node regenerated into four nodes in $S$, as is locally depicted in Figure 17, consider the resulting braid from this regeneration and the resulting braid from the regeneration of the singularity in $r(S)$. Then these braids are related by a rotation around a vertical line.*

*Proof.* Suppose that in $S$ the indices of the lines are $i$ and $j$; by Proposition 20 we may take $j = i+1$. Then the resulting braid is $Z^2_{i\ i'\ j\ j'}$, which by Proposition 13 and Property 1 gives

$$(5.7)\qquad Z^2_{i'\ j'}Z^2_{i'\ j}Z^2_{i\ j'}Z^2_{i\ j} = (\sigma_{2i+1}^{-1}\sigma_{2i}^2\sigma_{2i+1})(\sigma_{2i}^2)(\sigma_{2i+1}^{-1}\sigma_{2i}^{-1}\sigma_{2i-1}^2\sigma_{2i}\sigma_{2i+1})(\sigma_{2i}^{-1}\sigma_{2i-1}^2\sigma_{2i}).$$

This simplifies to $\sigma_{2i}\sigma_{2i-1}\sigma_{2i+1}\sigma_{2i}^2\sigma_{2i-1}\sigma_{2i+1}\sigma_{2i}$.

In the rotation $r(S)$ the indices of the lines are $(n+1)-j = (n+1)-(i+1) = (n-i)$ and $(n+1)-i = (n-i+1)$. Then the resulting braid is $Z^2_{(n-i)\ (n-i)'\ (n-i+1)\ (n-i+1)'}$, which by Proposition 13 and Property 1 simplifies to $\sigma_{2(n-i)}\sigma_{2(n-i)+1}\sigma_{2(n-i)-1}\sigma_{2(n-i)}^2\sigma_{2(n-i)+1}\sigma_{2(n-i)-1}\sigma_{2(n-i)}$.

Then it is clear that these two simplifications are related by a rotation around a vertical line with $\sigma_{2i}$ rotated to $\sigma_{2n-(2i)} = \sigma_{2(n-i)}$, $\sigma_{2i-1}$ rotated to $\sigma_{2n-(2i-1)} = \sigma_{2(n-i)+1}$, and $\sigma_{2i+1}$ rotated to $\sigma_{2n-(2i+1)} = \sigma_{2(n-i)-1}$. ☐

**Lemma 29.** *For the case of a tangency regenerated into three cusps in $S$, as is locally depicted in Figure 20, consider the resulting braid from this regeneration and the resulting braid from the regeneration of the singularity in $r(S)$. Then these braids are related by a rotation around a vertical line.*

*Proof.* Suppose that in $S$ the index $i$ of the conic is less than the index $j$ of the line as in Figure 20 (A). By Proposition 20 we may take $j = i+1$. Then the resulting braid is $Z^3_{i'\ j\ j'}$, which by Proposition 22 can be written as in Equation 5.1 using the regeneration rule for tangency (Theorem 14). This simplifies to $\sigma_{2i}\sigma_{2i+1}^3\sigma_{2i}\sigma_{2i+1}^3\sigma_{2i}$.

In the rotation $r(S)$ the index $(n+1)-j = (n+1)-(i+1) = (n-i)$ of the line is less than the index $(n+1)-i = (n-i+1)$ of the conic as in Figure 20 (B). Then the resulting braid is $Z^3_{(n-i)\ (n-i)'\ (n-i+1)}$, which by Proposition 22 can be written as in Equation 5.3 using the regeneration rule for tangency (Theorem 14). This simplifies to $\sigma_{2(n-i)}\sigma_{2(n-i)-1}^3\sigma_{2(n-i)}\sigma_{2(n-i)-1}^3\sigma_{2(n-i)}$.

Then it is clear that Equations 5.1 and 5.3 are related by a rotation around a vertical line with $\sigma_{2i}$ rotated to $\sigma_{2n-(2i)} = \sigma_{2(n-i)}$ and $\sigma_{2i+1}$ rotated to $\sigma_{2n-(2i+1)} = \sigma_{2(n-i)-1}$. ☐

Finally if the braids are related by a rotation around a vertical line, then the closures of these braids are the same links. ☐

## 6. EXAMPLES

In this section the three main examples we will consider will come from 2-points and 3-points. We exhibit their braid monodromies and give some properties of their closures as links.

*Example-Proposition* 30. The closure of the braid for the complete regeneration for a 2-point is a two-component link where each component is itself unknotted and the two components have linking number four.

*Proof.* By Proposition 22, the braid for the complete regeneration for a 2-point is

$$\sigma_2\sigma_3^2\sigma_2(\sigma_1\sigma_3)\sigma_2\sigma_3^2\sigma_2 \tag{6.1}$$

for the partial regeneration given in Figure 20 (A) and

$$\sigma_2\sigma_1^2\sigma_2(\sigma_1\sigma_3)\sigma_2\sigma_1^2\sigma_2 \tag{6.2}$$

for the partial regeneration given in Figure 20 (B). We depict these braids horizontally in Figure 30.

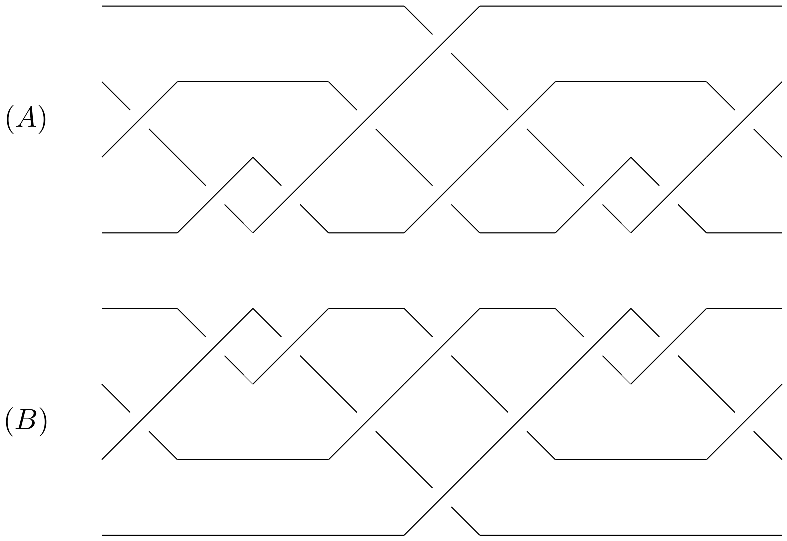

Figure 30. The braids for the complete regeneration for a 2-point given in Equations (A) 6.1 and (B) 6.2.

These braids are related by rotation around a line parallel to the direction of the braid (horizontally in the figure), and thus the closures give the same link by Proposition 27. Thus we only consider Figure 20 (A) where the conic is labelled by $i$ and $i'$ and the line is labelled by $j$. However, this is only a partial regeneration; in the complete regeneration the line becomes two lines $j$ and $j'$.

Via Proposition 20 we may associate these four components to strands in the braid.

By Lemma 24, the branch point of the conic contributes a single component to the link because the two strands labelled by $i$ and $i'$ are twisted by $Z_{i\,i'}$. See Figure 31 for one of these braids depicted horizontally.

By Lemma 25, the tangency twists the two strands $j$ and $j'$ with $Z_{j\,j'}$, creating a single component for the line. Furthermore, the tangency links the $i'$-th strand with both strands $j$ and $j'$ giving a linking number of four total. See Figure 32 for one of these braids depicted horizontally.

The link may be stabilized to get rid of the first strand resulting in $\sigma_1\sigma_2^2\sigma_1\sigma_2\sigma_1\sigma_2^2\sigma_1$ and its rotation.

In particular, this link is L4a1 where one component is replaced by its (2,1)-cable. ☐

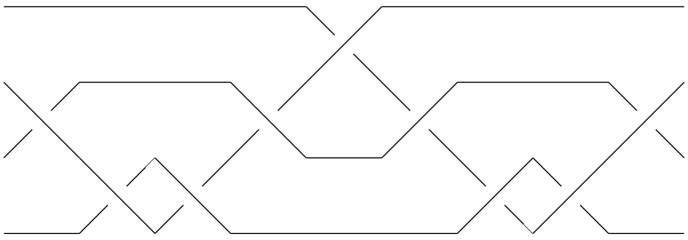

Figure 31. One of the braids obtained from the regeneration of a branch point as in Lemma 24 and Figure 21 (A2).

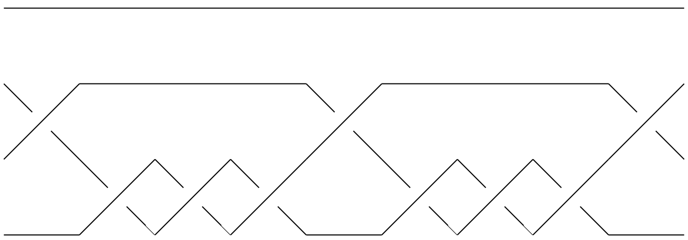

Figure 32. One of the braids obtained from the regeneration of a tangency as in Lemma 25 and Figure 21 (A1).

*Remark* 31. Recall Proposition 16 (A) above in which we considered the partial regeneration for a line tangent to a conic. There we obtained the link L4a1 without the cabling.

*Example-Proposition* 32. The closure of the braid for the complete regeneration for a 3-point of the first type is a three-component link where each component is itself unknotted and each pair of components has linking number four.

*Proof.* Recall that for a 3-point of the first type there are three cases as in Figure 25, where the singularities are ordered.

By Proposition 20 we may take $(i, j, k) = (1, 2, 3)$.

Then in the first case (A), the four singularities give, respectively, local contributions as follows:

(1) $\sigma_4^3(\sigma_4^{-1}\sigma_3^3\sigma_4)(\sigma_3^2\sigma_4^3\sigma_3^{-2})$
(2) $(\sigma_4^{-2}\sigma_3^{-1}\sigma_2^2\sigma_3\sigma_4^2)(\sigma_3\sigma_4^{-2}\sigma_3^{-1}\sigma_2^2\sigma_3\sigma_4^2\sigma_3^{-1})(\sigma_4^{-2}\sigma_3^{-1}\sigma_2^{-1}\sigma_1^2\sigma_2\sigma_3\sigma_4^2)(\sigma_3\sigma_4^{-2}\sigma_3^{-1}\sigma_2^{-1}\sigma_1^2\sigma_2\sigma_3\sigma_4^2\sigma_3^{-1})$
(3) $(\sigma_4^{-1}\sigma_3^{-1}\sigma_2^3\sigma_3\sigma_4)(\sigma_4^{-1}\sigma_3^{-1}\sigma_2^{-1}\sigma_1^3\sigma_2\sigma_3\sigma_4)(\sigma_1^2\sigma_4^{-1}\sigma_3^{-1}\sigma_2^3\sigma_3\sigma_4\sigma_1^{-2})$
(4) $\sigma_4^{-1}\sigma_3^{-1}\sigma_2^{-1}\sigma_1^{-2}\sigma_2^{-1}\sigma_3^{-1}\sigma_4^{-1}\sigma_5\sigma_4\sigma_3\sigma_2\sigma_1^2\sigma_2\sigma_3\sigma_4$

In the second case (B), we have:

(1) $\sigma_2^3(\sigma_2^{-1}\sigma_1^3\sigma_2)(\sigma_1^2\sigma_2^3\sigma_1^{-2})$
(2) $(\sigma_5^{-1}\sigma_4^3\sigma_5)\sigma_4^3(\sigma_5\sigma_4^3\sigma_5^{-1})$
(3) $\sigma_4^{-1}\sigma_5^{-2}\sigma_4^{-1}\sigma_2^{-1}\sigma_1^{-2}\sigma_2^{-1}\sigma_3\sigma_2\sigma_1^2\sigma_2\sigma_4\sigma_5^2\sigma_4$
(4) $(\sigma_5^{-1}\sigma_4^{-1}\sigma_3\sigma_2^2\sigma_3^{-1}\sigma_4\sigma_5)(\sigma_4^{-1}\sigma_3\sigma_2^2\sigma_3^{-1}\sigma_4)(\sigma_5^{-1}\sigma_4^{-1}\sigma_3\sigma_2^{-1}\sigma_1^2\sigma_2\sigma_3^{-1}\sigma_4\sigma_5)(\sigma_4^{-1}\sigma_3\sigma_2^{-1}\sigma_1^2\sigma_2\sigma_3^{-1}\sigma_4)$

And in the third case (C), we have:

(1) $(\sigma_3^{-1}\sigma_2^3\sigma_3)\sigma_2^3(\sigma_3\sigma_2^3\sigma_3^{-1})$
(2) $(\sigma_5^{-1}\sigma_3\sigma_2^{-2}\sigma_3^{-1}\sigma_4^2\sigma_3\sigma_2^2\sigma_3^{-1}\sigma_5)(\sigma_3\sigma_2^{-2}\sigma_3^{-1}\sigma_4^2\sigma_3\sigma_2^2\sigma_3^{-1})(\sigma_5^{-1}\sigma_3^2\sigma_2^{-2}\sigma_3^{-1}\sigma_4^2\sigma_3\sigma_2^2\sigma_3^{-2}\sigma_5)(\sigma_3^2\sigma_2^{-2}\sigma_3^{-1}\sigma_4^2\sigma_3\sigma_2^2\sigma_3^{-2})$
(3) $(\sigma_5^{-1}\sigma_4\sigma_3\sigma_2^3\sigma_3^{-1}\sigma_4^{-1}\sigma_5)(\sigma_4\sigma_3\sigma_2^3\sigma_3^{-1}\sigma_4^{-1})(\sigma_5\sigma_4\sigma_3\sigma_2^3\sigma_3^{-1}\sigma_4^{-1}\sigma_5^{-1})$
(4) $\sigma_2^{-1}\sigma_3^{-1}\sigma_4^{-1}\sigma_5^{-2}\sigma_4^{-1}\sigma_3^{-1}\sigma_2^{-1}\sigma_1\sigma_2\sigma_3\sigma_4\sigma_5^2\sigma_4\sigma_3\sigma_2$

The simplification for (A) is a word of length 27 with all its generators positive:

$$\sigma_4\sigma_3^2\sigma_4\sigma_2\sigma_3\sigma_1\sigma_2\sigma_4\sigma_3^2\sigma_2(\sigma_4\sigma_3\sigma_2\sigma_1)\sigma_2\sigma_3(\sigma_5\sigma_4\sigma_3\sigma_2\sigma_1)(\sigma_1\sigma_2\sigma_3\sigma_4).$$

The simplification for (B) is also a word of length 27 with all its generators positive:

$$(\sigma_4\sigma_3\sigma_2\sigma_1)(\sigma_5\sigma_4\sigma_3\sigma_2)(\sigma_1\sigma_2\sigma_3\sigma_4\sigma_5)(\sigma_1\sigma_2\sigma_3\sigma_4)(\sigma_3\sigma_2\sigma_1\sigma_3\sigma_2\sigma_3\sigma_2\sigma_1\sigma_3\sigma_2).$$

The braid in (C) is related by rotation around a line parallel with the braid to the braid in (A), and thus the closures give the same link by Proposition 27.

Via Proposition 20 we may associate the six components to six strands in the braid. By Lemma 24, the branch point of the conic contributes a single component to the link. By Lemma 25, each tangency contributes a single component for the relevant line and links the conic with this line giving a linking number of four total. By Lemma 26, the node on the two lines links the two line components giving a linking number of four total.

The closures of (A) and (B) are in fact the same link; this can be given by the torus link $T(3,3)$ with each component replaced by its $(2,1)$-cable. ☐

*Example-Proposition* 33. The closure of the braid for the complete regeneration for a 3-point of the second type is a four-component link where each component is itself unknotted, whose linking numbers are given by the following matrix:

$$\begin{pmatrix} & 1 & 2 & 2 \\ 1 & & 2 & 2 \\ 2 & 2 & & 4 \\ 2 & 2 & 4 & \end{pmatrix}. \tag{6.3}$$

*Proof.* Recall that for a 3-point of the second type there is just a single case as in Figure 15. The first two singularities give three cusps and a branch point, the next gives four nodes, and the last two give another three cusps and a branch point.

By Proposition 20 we may take $(i,j,k) = (1,2,3)$.

Then the singularities give, respectively, local contributions as follows:

(1) $\sigma_4^3(\sigma_4^{-1}\sigma_3^3\sigma_4)(\sigma_3^2\sigma_4^3\sigma_3^{-2})$
(2) $\sigma_4^{-1}\sigma_3^{-2}\sigma_4^{-1}\sigma_5\sigma_4\sigma_3^2\sigma_4$
(3) $(\sigma_5^{-1}\sigma_4^{-1}\sigma_3^{-1}\sigma_2^2\sigma_3\sigma_4\sigma_5)(\sigma_5^{-1}\sigma_4^{-1}\sigma_3^{-1}\sigma_2^{-1}\sigma_1^2\sigma_2\sigma_3\sigma_4\sigma_5)$
$(\sigma_4^{-1}\sigma_3^{-2}\sigma_4^{-2}\sigma_3^{-1}\sigma_2^2\sigma_3\sigma_4^2\sigma_3^2\sigma_4)(\sigma_4^{-1}\sigma_3^{-2}\sigma_4^{-2}\sigma_3^{-1}\sigma_2^{-1}\sigma_1^2\sigma_2\sigma_3\sigma_4^2\sigma_3^2\sigma_4)$
(4) $(\sigma_3^{-1}\sigma_2^3\sigma_3)\sigma_2^3(\sigma_3\sigma_2^3\sigma_3^{-1})$
(5) $\sigma_2^{-1}\sigma_3^{-2}\sigma_2^{-1}\sigma_1\sigma_2\sigma_3^2\sigma_2$

The simplification is a word of length 28 with all its generators positive:

$$\sigma_1\sigma_2\sigma_5\sigma_4\sigma_3\sigma_5\sigma_2\sigma_3\sigma_1\sigma_2(\sigma_2\sigma_3\sigma_4\sigma_5)\sigma_5\sigma_4^2\sigma_5\sigma_3\sigma_4^2\sigma_3\sigma_4\sigma_2\sigma_3\sigma_4^2\sigma_3.$$

Via Proposition 20 we may associate the six components to six strands in the braid. By Lemma 24, the branch points of the two conics each contributes a single component to the link. By Lemma 25, each tangency contributes a single half-twist on the two components associated to the line, giving a single full-twist of the two strands associated to the line, linking each of these components with each of the conic components twice. This accounts for singularities (1), (2), (4), and (5) on the list above.

The remaining singularity does not actually appear in the partial regeneration shown in Figure 15. This is a node at which the conics intersect, and we apply the regeneration rule for a node Theorem12. By Lemma 26 this gives links the two conic components with linking number four.

This link is the torus link $T(3,3)$ with two strands (associated with the conics) replaced by their $(2,1)$-cables and one strand (associated with the line) replaced by its $(2,2)$-cable. ☐

These last two examples lead to the obvious conclusion.

**Corollary 34.** *The 3-points of the first type and the 3-points of the second type give different braids.*

## ACKNOWLEDGMENTS

This work was supported in part by the Edmund Landau Center for Research in Mathematics, the Emmy Noether Research Institute for Mathematics, the Minerva Foundation (Germany), the EU-network HPRN-CT-2009-00099(EAGER), the Israel Science Foundation grant # 8008/02-3 (Excellency Center "Group Theoretic Methods in the Study of Algebraic Varieties"), and the Oswald Veblen Fund.

## REFERENCES

[1] M. Amram, C. Ciliberto, R. Miranda, and M. Teicher. Braid monodromy factorization for a non-prime $K3$ surface branch curve. *Israel J. Math.*, 170:61–93, 2009.

[2] M. Amram, M. Friedman, and M. Teicher. The fundamental group of the complement of the branch curve of $\mathbb{CP}^1 \times T$. *Acta Math. Sin. (Engl. Ser.)*, 25(9):1443–1458, 2009.

[3] M. Amram, M. Friedman, and M. Teicher. The fundamental group of the complement of the branch curve of the second Hirzebruch surface. *Topology*, 48(1):23–40, 2009.

[4] M. Amram, D. Garber, R. Shwartz, and M. Teicher. 8-point - regenerations and applications. *Adv. in Geom. Anal.*, ALM21(4):307–342, 2012.

[5] M. Amram, D. Garber, and M. Teicher. Fundamental groups of tangent conic-line arrangements with singularities up to order 6. *Math. Z.*, 256(4):837–870, 2007.

[6] M. Amram, D. Garber, and M. Teicher. On the fundamental group of the complement of two tangent conics and an arbitrary number of tangent lines. 2012.

[7] M. Amram and D. Goldberg. Higher degree Galois covers of $\mathbb{CP}^1 \times T$. *Algebr. Geom. Topol.*, 4:841–860 (electronic), 2004.

[8] M. Amram, D. Goldberg, M. Teicher, and U. Vishne. The fundamental group of a Galois cover of $\mathbb{CP}^1 \times T$. *Algebr. Geom. Topol.*, 2:403–432 (electronic), 2002.

[9] M. Amram, R. Lehman, R. Shwartz, and M. Teicher. Classification of fundamental groups of Galois covers of surfaces of small degree degenerating to nice plane arrangements. In *Topology of algebraic varieties and singularities*, volume 538 of *Contemp. Math.*, pages 65–94. Amer. Math. Soc., Providence, RI, 2011.

[10] M. Amram and S. Ogata. Degenerations and fundamental groups related to some special toric varieties. *Michigan Math. J.*, 54(3):587–610, 2006.

[11] M. Amram and M. Teicher. The fundamental group of the complement of the branch curve of $T \times T$ in $\mathbb{C}^2$. *Osaka J. Math.*, 40(4):857–893, 2003.

[12] M. Amram and M. Teicher. On the degeneration, regeneration and braid monodromy of $T \times T$. *Acta Appl. Math.*, 75(1-3):195–270, 2003. Monodromy and differential equations (Moscow, 2001).

[13] M. Amram, M. Teicher, and A. M. Uludag. Fundamental groups of some quadric-line arrangements. *Topology Appl.*, 130(2):159–173, 2003.

[14] M. Amram, M. Teicher, and U. Vishne. The fundamental group of the Galois cover of Hirzebruch surface $F_1(2, 2)$. *Internat. J. Algebra Comput.*, 17(3):507–525, 2007.

[15] M. Amram, M. Teicher, and U. Vishne. The fundamental group of Galois cover of the surface $T \times T$. *Internat. J. Algebra Comput.*, 18(8):1259–1282, 2008.

[16] E. Artin. Theory of braids. *Ann. of Math. (2)*, 48:101–126, 1947.

[17] D. Bar-Natan, S. Morrison, and et al. The Knot Atlas. http://katlas.org.

[18] C. Ciliberto, R. Miranda, and M. Teicher. Pillow degenerations of $K3$ surfaces. In *Applications of algebraic geometry to coding theory, physics and computation (Eilat, 2001)*, volume 36 of *NATO Sci. Ser. II Math. Phys. Chem.*, pages 53–63. Kluwer Acad. Publ., Dordrecht, 2001.

[19] M. Friedman and M. Teicher. The regeneration of a 5-point. *Pure Appl. Math. Q.*, 4(2, Special Issue: In honor of Fedor Bogomolov. Part 1):383–425, 2008.

[20] D. Garber, M. Teicher, and U. Vishne. Classes of wiring diagrams and their invariants. *J. Knot Theory Ramifications*, 11(8):1165–1191, 2002.

[21] C. Kassel and V. Turaev. *Braid groups*, volume 247 of *Graduate Texts in Mathematics*. Springer, New York, 2008. With the graphical assistance of Olivier Dodane.

[22] B. Moishezon and M. Teicher. Simply-connected algebraic surfaces of positive index. *Invent. Math.*, 89(3):601–643, 1987.

[23] B. Moishezon and M. Teicher. Braid group technique in complex geometry. I. Line arrangements in $\mathbb{CP}^2$. In *Braids (Santa Cruz, CA, 1986)*, volume 78 of *Contemp. Math.*, pages 425–555. Amer. Math. Soc., Providence, RI, 1988.

[24] B. Moishezon and M. Teicher. Braid group technique in complex geometry. II. From arrangements of lines and conics to cuspidal curves. In *Algebraic geometry (Chicago, IL, 1989)*, volume 1479 of *Lecture Notes in Math.*, pages 131–180. Springer, Berlin, 1991.

[25] B. Moishezon and M. Teicher. Braid group techniques in complex geometry. III. Projective degeneration of $V_3$. In *Classification of algebraic varieties (L'Aquila, 1992)*, volume 162 of *Contemp. Math.*, pages 313–332. Amer. Math. Soc., Providence, RI, 1994.

[26] B. Moishezon and M. Teicher. Braid group techniques in complex geometry. IV. Braid monodromy of the branch curve $S_3$ of $V_3 \to \mathbb{CP}^2$ and application to $\pi_1(\mathbb{CP}^2 - S_3, *)$. In *Classification of algebraic varieties (L'Aquila, 1992)*, volume 162 of *Contemp. Math.*, pages 333–358. Amer. Math. Soc., Providence, RI, 1994.

[27] B. Moishezon and M. Teicher. Braid group technique in complex geometry. V. The fundamental group of a complement of a branch curve of a Veronese generic projection. *Comm. Anal. Geom.*, 4(1-2):1–120, 1996.

Department of Mathematics, Bar-Ilan University, Ramat-Gan, 52900, Israel
and Shamoon College of Engineering, Bialik/Basel Sts., Beer-Sheva 84100, Israel

Department of Mathematics, Bar-Ilan University, Ramat Gan 52900, Israel

Department of Mathematics, Bar-Ilan University, Ramat Gan 52900, Israel